Carl D. Meinhart
Assistant Professor,
Department of Mechanical
& Environmental Engineering,
University of California,
Santa Barbara, CA 93106
e-mail: meinhart@engineering.vcsb.edu

Steve T. Wereley
Assistant Professor,
Mechanical Engineering,
Purdue University,
1288 Mechanical Engineering Building,
West Lafayette, IN 47909-1288

Juan G. Santiago
Assistant Professor,
Department of Mechanical Engineering,
Stanford University,
Stanford, CA 94305-3030

A PIV Algorithm for Estimating Time-Averaged Velocity Fields

A PIV algorithm is presented for estimating time-averaged or phase-averaged velocity fields. The algorithm can be applied to situations where signal strength is not sufficient for standard cross correlation techniques, such as a low number of particle images in an interrogation spot, or poor image quality. The algorithm can also be used to increase the spatial resolution of measurements by allowing smaller interrogation spots than those required for standard cross correlation techniques. The quality of the velocity measurements can be dramatically increased by averaging a series of instantaneous correlation functions, before determining the location of the signal peak, as opposed to the commonly used technique of estimating instantaneous velocity fields first and then averaging the velocity fields. The algorithm is applied to a 30 μm$\times$300 μm microchannel flow.
[S0098-2202(00)00602-7]

1 Introduction

There has been a significant amount of work over the past 15 years developing theory for particle image velocimetry, including Adrian and Yao [1], Adrian [2,3], Keane and Adrian [4,5], and Westerweel [6]. A large fraction of this effort has been focused on determining optimal conditions for measuring instantaneous velocity information, and understanding the performance of the instrument under a variety of operating conditions. One key advantage of the PIV technique over other conventional techniques such as LDV or hotwire anemometry is the ability to obtain instantaneous full-field velocity information. This instantaneous flow-field information is important for probing the structure of turbulent flow fields (Westerweel, et al. [7], Meinhart and Adrian [8]).

Recently, micro-PIV techniques have been developed to measure flows in microfluidic devices with spatial resolutions on the order of several microns (Santiago et al. [9] and Meinhart et al. [10]). At the microscale, it is difficult to form a light sheet that is only a few microns thick, and even more difficult to align such a light sheet with the objective plane of the recording optics. Therefore, in micro-PIV experiments, the entire test section volume is illuminated with a cone of light emanating from the recording lens, instead of a commonly used light sheet. This limits the number density of particles that can be used to trace the flow. If the particle density is too high, then background noise from out-of-focus particles will dominate the image and reduce the visibility of in-focus particles. If the particle density is too low, then standard cross correlation techniques will fail to provide an adequate signal, causing the measurements to be noisy and sometimes unreliable.

Since many of the low Reynolds number flows in microfluidic devices are laminar and either steady or periodic, it is not necessary to determine instantaneous velocity information. For many of these flows, it is sufficient to measure only the time-averaged or phase-averaged velocity field. In principle, these flow fields can be measured using high-resolution pointwise techniques such as the dual beam laser Doppler anemometer (LDA) system developed by Tieu, Machenzie and Li [11]. This LDA system uses low *f-number* optics to focus the probe volume down to approximately 5 μm$\times$10 μm. The micron-resolution LDA technique has advantages over the micro-PIV technique in that one does not have to deal with out of focus particle images, and that one can obtain large numbers of velocity measurements in real time. Micro PIV has advantages over micro LDA in that it does not require alignment of laser beams inside a microfluidic device, and it does require sweeping the probe volume throughout the measurement domain. In addition, micro PIV takes advantage of the high signal to noise levels offered by fluorescence imaging.

In this paper, we present a PIV algorithm that directly estimates time-averaged or phase-averaged velocity fields. The algorithm can provide reliable measurements in low signal-to-noise conditions where standard cross correlation techniques fail. The PIV algorithm is demonstrated by measuring flow in a 30 μm $\times$300 μm microchannel flow.

2 Decomposition of the Correlation Function

The auto correlation function of a single-frame double-exposure particle image field, $I(\mathbf{X})$, is defined as

$$R(\mathbf{s}) = \int\int I(\mathbf{X})I(\mathbf{X}+\mathbf{s})d^2\mathbf{X}, \tag{1}$$

where $\mathbf{X}$ is the spatial coordinate in the image plane and $\mathbf{s}$ is the spatial coordinate in the correlation plane.

$R(\mathbf{s})$ can be decomposed into the following components

$$R(\mathbf{s}) = R_C(\mathbf{s}) + R_P(\mathbf{s}) + R_F(\mathbf{s}) + R_{D^-}(\mathbf{s}) + R_{D^+}(\mathbf{s}), \tag{2}$$

where R_C is the convolution of mean image intensity, R_P is the pedestal component resulting from each particle image correlating with itself, and R_F is the fluctuating component resulting from the correlation between fluctuating image intensity with mean image intensity (Adrian [2]). The positive and negative displacement components are R_{D^+} and R_{D^-}, respectively.

The signal used to measure displacement is contained only in the R_{D^+} component. Consequently, contributions from all other components of the correlation function may bias the measurements, add random noise to the measurements, or even cause erroneous measurements. Therefore, it is desirable to reduce or eliminate all the other components. If both exposures of a double-pulse particle image field are recorded separately as a double-frame image field, then the particle images can be interrogated using cross correlation (Keane and Adrian [5]). In the case of

Contributed by the Fluids Engineering Division for publication in the JOURNAL OF FLUIDS ENGINEERING. Manuscript received by the Fluids Engineering Division May 17, 1999; revised manuscript received February 2, 2000. Associate Technical Editor: S. Banerjee.

double-frame cross correlation, the R_P and R_{D^-} components do not exist. Further improvements in signal quality can be obtained by image processing. By subtracting the mean image intensity at each interrogation spot before correlation, the R_C and $R_F(s)$ components are set identically to zero, leaving only the positive displacement component, R_{D^+}, in the correlation function.

While the R_{D^+} component is commonly considered the signal component, it contains both noise and signal information. In order to make accurate measurements, the signal-to-noise ratio in the R_{D^+} component must be sufficiently high. This paper presents a method in which the signal-to-noise ratio can be increased when one is interested in measuring average displacement fields.

3 Methods of Estimating Average Velocity Fields

Average velocity fields can be obtained by first measuring instantaneous velocities and then averaging them in either space or time. Here we present an alternative method for measuring average velocity fields directly from the correlation function.

Estimation of velocity-vector fields using PIV involves three primary steps:

1 Particle Image Acquisition
2 Particle Image Correlation
3 Correlation Peak Detection

In order to obtain an average velocity measurement, one must apply an averaging operation. The averaging operator is a linear operator, and can be applied after step (1), step (2), or step (3), to produce a nonbiased estimate of average velocity. The particle-image correlation and peak detection operations are both nonlinear, and the order in which the averaging operator is applied can dramatically change the quality of the resulting signal.

In this section, we examine the three different methods for calculating average velocities based upon the order in which the averaging operator is applied. Here we assume that two single exposure images, *Image A* and *Image B*, are separated by a known time delay, Δt, and represent the image acquisition of a single realization. Furthermore, a sequence of two image pairs is acquired at N different realizations of a statistically stationary process. We wish to average over the N realizations to estimate the average velocity.

3.1 Average Velocity Method. In this method, the estimate of the average velocity is determined by (1) correlating *Image A* and *Image B*, (2) detecting the peak from the instantaneous correlation functions, and (3) averaging over the instantaneous velocity measurements. Figure 1(*a*) graphically depicts this process. The primary advantage of this method is that one can obtain instantaneous velocity measurements, which may be of physical importance. However, if one is primarily interested in the average velocity field, this method may not be optimal.

The nonlinear operation of peak detection is susceptible to producing erroneous measurements when the signal to noise is low in the instantaneous correlation. In practice, the vector fields must be validated by identifying and removing erroneous velocity measurements (Meinhart et al. [12], Westerweel [13]). Without vector validation, all the instantaneous measurements must be reliable in order to obtain a reliable average velocity measurement. For situations where the particle image density is low, there may not be adequate signal to obtain valid measurements from the instantaneous correlation functions. In these situations, the alternative methods described below may be employed.

3.2 Average Image Method. In this method, the averaging operation is applied directly on image fields A and B, and then correlated to obtain $R_{\overline{A}\overline{B}}$. This process is depicted graphically in Fig. 1(*b*). In the situation where particle image number density is low, averaging the image fields together can increase the average number of particles per interrogation spot. However, excessive

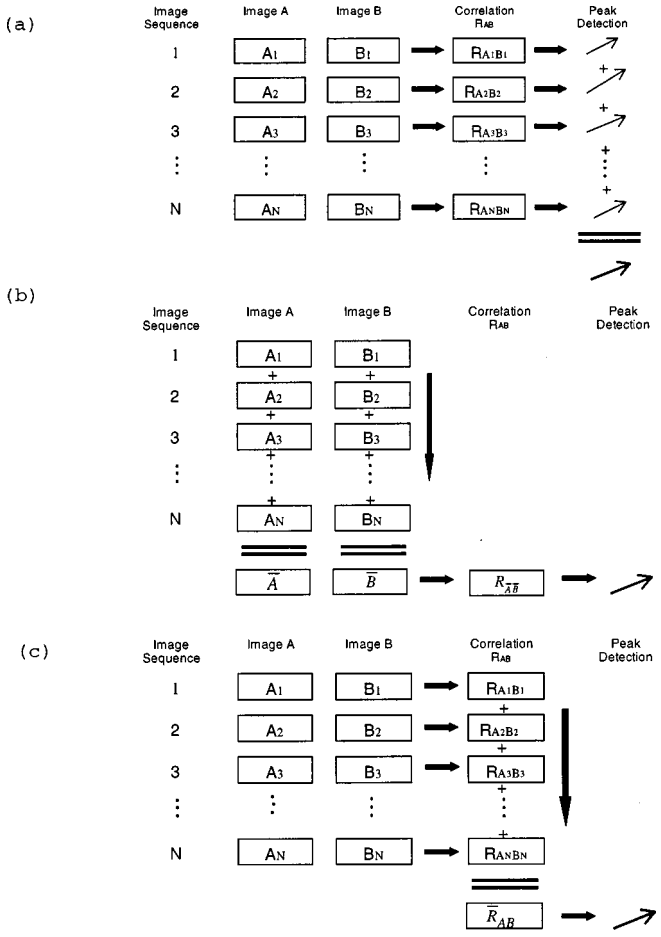

Fig. 1 Diagrams depicting the different ways in which the average velocity can be estimated: (*a*) average velocity method, (*b*) average image method, (*c*) average correlation method

averaging of the image fields can create too many particle images in the interrogation spot and reduce the visibility of individual particle images.

The 2-D spatial correlation function of the average of A and B image fields is defined as

$$R_{\overline{A}\overline{B}}(\mathbf{s}) = \int \int \overline{A}(\mathbf{X})\overline{B}(\mathbf{X}+\mathbf{s})d^2\mathbf{X}, \tag{3}$$

where $\overline{A} = 1/N\Sigma_{i=1}^{N} A_i$ is the average operator, averaging over N realizations of the flow field. Expanding the integrand of (3) yields

$$R_{\overline{A}\overline{B}}(s) = \int \int \begin{bmatrix} A_1B_1 + A_1B_2 + A_1B_3 + \cdots + A_1B_N + \\ A_2B_1 + A_2B_2 + A_2B_3 + \cdots + A_2B_N + \\ A_3B_1 + A_3B_2 + A_3B_3 + \cdots + A_3B_N + \\ \cdot \quad\quad\quad \cdot \quad\quad \cdot \\ \cdot \quad\quad\quad\quad \cdot \quad \cdot \\ \cdot \quad\quad\quad\quad\quad \cdot \quad \cdot \\ A_NB_1 + A_NB_2 + A_NB_3 + \cdots + A_NB_N \end{bmatrix} d^2\mathbf{X}. \tag{4}$$

Following the discussion in the previous section, if A and B represent paired single-exposure image fields separated by a known time interval, Δt, which are cross correlated, and if the mean image intensity is subtracted before correlation, then all $N \times N$ terms in (4) are contained in the R_{D^+} component of R.

Only the N diagonal terms in (4) contribute to signal. The $N(N-1)$ off diagonal terms represent random particle correlation

across different realizations, which produce noise in the correlation function that can reduce the accuracy of the measurement and cause erroneous measurements. Since the off diagonal terms are random and uniformly distributed throughout the correlation plane, they may or may not contaminate the signal peak. The number of noise terms increases as N^2, while the number of signal terms increases as N.

In demanding situations when particle-number density is low, or when small interrogation regions are chosen to produce high spatial resolution, it may be impossible to obtain an adequate signal from instantaneous cross correlation analysis. Clearly, averaging the particle-image fields over several realizations and then correlating can increase the signal-to-noise ratio. However, if the number of realizations used in the average is beyond an optimal number, the signal-to-noise ratio can be reduced by further increases in N. Loss of signal occurs because the number of nondiagonal (noise) terms increases faster than the diagonal (signal) terms. The optimal number of realizations depends upon many factors including, interrogation spot size, particle-image number density, and particle-image quality.

3.3 Average Correlation Method. A third method for estimating average displacement fields is to calculate instantaneous correlation functions, average the correlation function, and then determine the location of the signal peak location. The *Average Correlation Method*, is shown graphically in Fig. 1(*c*). The average of instantaneous correlation functions over N realizations can be written as

$$\overline{R}_{AB}(s)=\overline{\int\int A(\mathbf{X})B(\mathbf{X}+\mathbf{s})d^2\mathbf{X}}=\int\int \overline{A(\mathbf{X})B(\mathbf{X}+\mathbf{s})}d^2\mathbf{X}. \tag{5}$$

Figure 2 shows several instantaneous correlation functions, and an average correlation function calculated by averaging 20 instantaneous correlation functions. The instantaneous correlation functions are characteristic of micro-PIV data and were obtained from an actual micro-PIV experiment. The instantaneous correlation functions contain significant amounts of noise that can lead to inaccurate or unreliable measurements. This noise is substantially less in the average correlation function.

Since the operations of averaging and integration commute, the average operator can be taken inside of the integral so that

$$\overline{R}_{AB}(\mathbf{s})=\int\int [A_1B_1+A_2B_2+A_3B_3+\cdots+A_NB_N]d^2\mathbf{X}. \tag{6}$$

From (6), the average correlation function contains only the diagonal (i.e., signal) terms of (4). Therefore, this type of average produces a much higher signal-to-noise ratio than the alternative methods that have been discussed previously. The number of signal terms increases linearly with the number of realizations, N. Unlike the average image method, there is no penalty for including large numbers of realizations in the average. Since the average operator is applied to the correlation function before peak detection, the probability of erroneous measurements is greatly reduced.

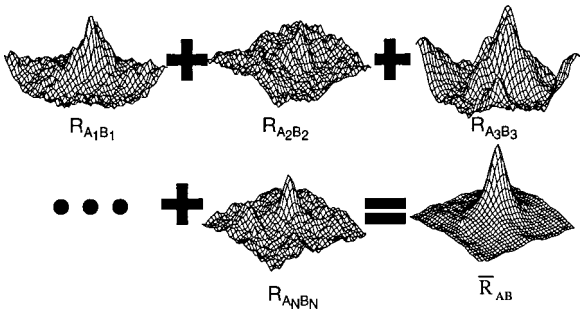

Fig. 2 Instantaneous cross correlation functions that are averaged together to produce an average correlation function. The average correlation function has a much higher signal-to-noise ratio than the instantaneous correlation functions.

4 Application to Microchannel Flow

The three different averaging algorithms were applied to a series of particle image fields taken of steady Stokes' water flow through a $30\,\mu\text{m}\times 300\,\mu\text{m}$ glass microchannel. Details of the same experiment but for a different flow rate are discussed by Meinhart et al. [10]. The out of plane measurement resolution is related to the depth of field of the microscope optics, and is estimated to be approximately 1.8 μm. Based on the discussion of Santiago et al. [9], the error due to Brownian motion for a single particle is estimated to be less than 3 percent full-scale error. The interrogation spot size was 16×64 pixels and 24×72 pixels, for window 1 and window 2, respectively. The relative offset between the windows was adjusted adaptively to approximate the particle image displacement at each measurement location. The interrogation windows were chosen to be small and have a high aspect ratio to achieve high spatial resolution in the wall-normal direction.

The signal-to-noise ratio from standard correlation techniques was relatively low, because there was an average of only 2.5 particle images located in each 16×64 pixel interrogation window. The signal-to-noise ratio could be improved by increasing the size of the correlation windows, but with reduced spatial resolution. Alternatively, the particle concentration in the flow field could be increased, but that would increase the number of out of focus particles, and produce more background image noise.

Figure 3(*a*) shows an instantaneous velocity-vector field, calculated using a standard cross correlation technique without any type of vector validation or smoothing applied to the field. The velocity measurements contained in the row closest to the wall are not considered to be accurate, because part of their interrogation region lies outside the flow domain. The velocity measurements are noisy, and approximately 20 percent appear to be erroneous. An average over 20 instantaneous velocity fields is shown in Fig. 3(*b*). Averaging reduces small random noise in the instantaneous fields. However, the large errors associated with the erroneous measurements are not averaged out quickly. The application of vector validation algorithms can usually eliminate errors due to erroneous measurements producing accurate velocity measurements, however a priori knowledge of the flow field is required.

The same series of double-frame particle image fields were correlated, the correlation functions were averaged, and then the locations of the signal peaks in the correlation plane were determined, following the *average correlation method* depicted in Fig. 1(*c*). The resulting velocity-vector field is shown in Fig. 3(*c*). No vector validation or smoothing has been applied to this field. The field contains only 0.5–1 percent erroneous measurements and has less noise than the vector fields shown in Figs. 3(*a*) and 3(*b*).

The relative performance of the three averaging algorithms was quantitatively compared by varying the number of realizations used in the average, from one to twenty. The fraction of valid measurements for each average was determined by identifying the number of velocity measurements in which the streamwise component of velocity deviated by more than 10 percent from the known solution at each point. For this comparison, the known solution was the velocity vector field estimated by applying the average correlation technique to 20 realizations, and then smoothing the flow field.

Figure 4 shows the fraction of valid measurements for each of the three algorithms as a function of the number of realizations used in the average. The average correlation method better than performs the other two methods, and produces less than 0.5–1 percent erroneous measurements after averaging eight realizations. The average image method produces about 95 percent reliable velocity measurements, and reaches a maximum at four averages. Further increases in the number of realizations used to

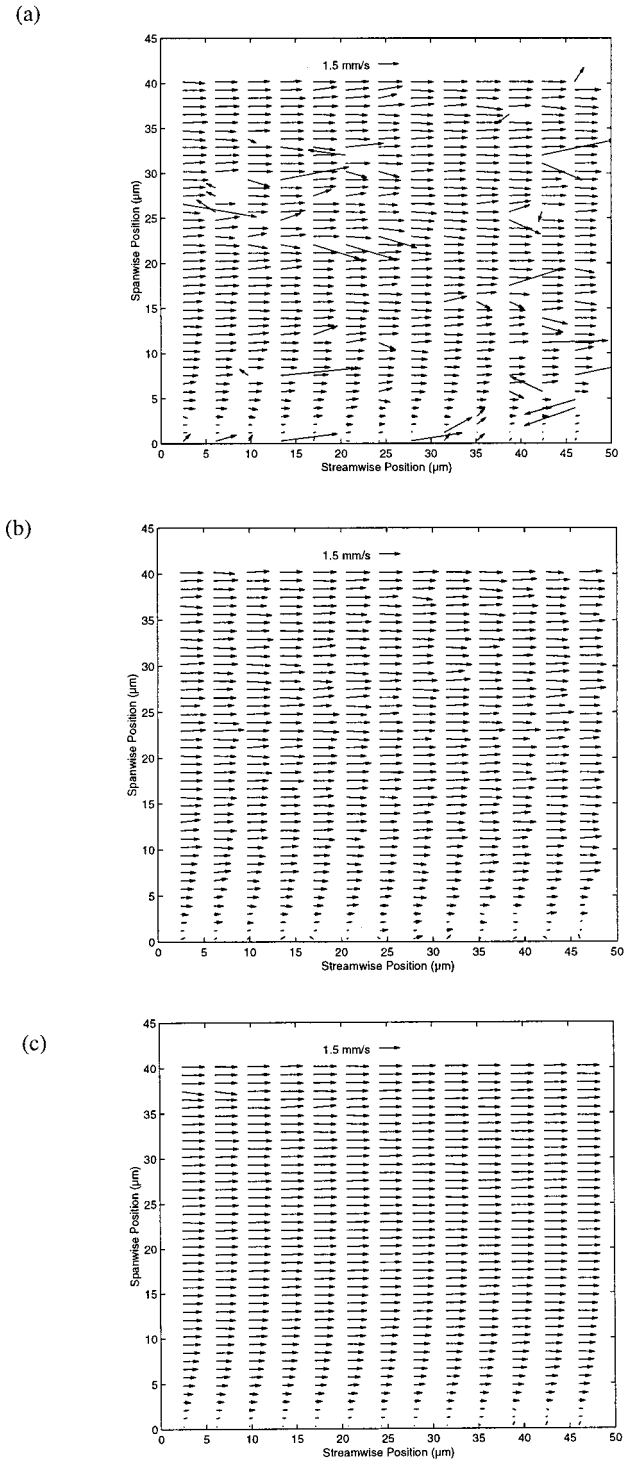

Fig. 3 Velocity vector fields showing the results from the different methods of calculation: (*a*) instantaneous velocity field, (*b*) time average of twenty instantaneous velocity fields, (*c*) velocity field calculated from time-averaged correlation functions

average the images decreases the signal to noise of the average particle-image field, and produces noise in the correlation plane due to random correlation between nonpaired particle images. The average velocity method reaches a maximum of 88 percent reliable measurements using two velocity averages. Further increases in the number of averages decreases the number of reliable measurements, due to an increase in the probability of an encountering an erroneous measurement.

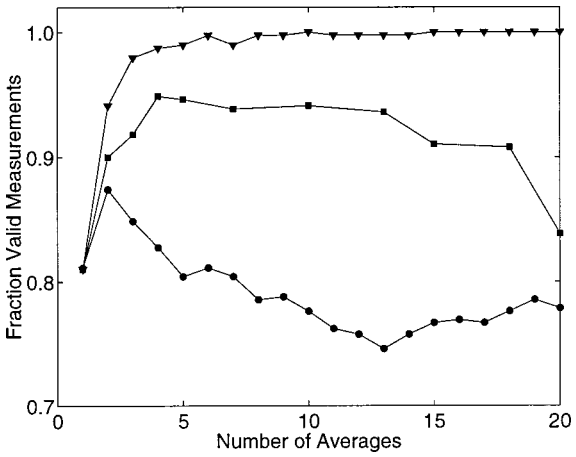

Fig. 4 Comparison of the performance of the three averaging techniques: average velocity ●, average image ■, and average correlation ▼

Conclusions

Three PIV algorithms are compared for estimated time-averaged velocity fields. The process of obtaining PIV measurements involves three primary steps: (1) particle image acquisition, (2) particle image correlation, and (3) correlation peak detection. In order to obtain average velocity fields, an averaging operator must be applied to the data. When signal strength is sufficient, the average can be applied after steps 1, 2, or 3. However, in demanding situations when signal strength is weak, the order in which the average operator is applied is important. The correlation and peak detection operators are nonlinear and do not commute with the average operator. Optimal signal strength can be achieved by first calculating instantaneous correlation functions, and then averaging the correlation functions before locating the signal peak.

The theoretical observations were confirmed by applying the three different algorithms to experimental particle image data from a 30 μm$\times$300 μm microchannel flow. The results showed that, by averaging instantaneous correlation functions before signal peak detection, high quality velocity data can be obtained with less than 0.5–1 percent erroneous measurements, even when only an average of 2.5 particle images were contained in a single interrogation spot.

Acknowledgments

This research is supported by AFOSR/DARPA F49620-97-1-0515, DARPA F33615-98-1-2853, and JPL/NASA 961270.

References

[1] Adrian, R. J., and Yao, C. S., 1985, ''Pulsed laser technique application to liquid and gaseous flows and the scattering power of seed materials,'' Appl. Opt., **24**, No. 1, pp. 44–52.
[2] Adrian, R. J., 1988, ''Double Exposure, Multiple-field particle image velocimetry for turbulent probability density,'' Opt. Lasers Eng., **9**, pp. 211–228.
[3] Adrian, R. J., 1991, ''Particle-imaging techniques for experimental fluid mechanics,'' Annu. Rev. Fluid Mech., **23**, pp. 261–304.
[4] Keane, R. D., and Adrian, R. J., 1991, ''Optimization of particle image velocimeters. II. Multiple pulsed systems,'' Meas. Sci. Technol., **2**, No. 10, Oct., pp. 963–974.
[5] Keane, R. D., and Adrian, R. J., 1992, ''Theory of cross-correlation analysis of PIV images,'' Appl. Sci. Res., **49**, pp. 191–215.
[6] Westerweel, J., 1997, ''Fundamentals of digital particle image velocimetry,'' Meas. Sci. Technol., **8**, pp. 1379–1392.
[7] Westerweel, J., Draad, A. A., van der Hoeven, J. G. Th., and van Oord, J., 1996, ''Measurement of fully developed turbulent pipe flow with digital PIV,'' Exp. Fluids, **20**, pp. 165–177.
[8] Meinhart, C. D., and Adrian, R. J., 1995, ''On the existence of uniform momentum zones in a turbulent boundary layer,'' Phys. Fluids, **7**, No. 4, pp. 694–696.
[9] Santiago, J. G., Wereley, S. T., Meinhart, C. D., Beebe, D. J., and Adrian, R.

J., 1998, ''A micro particle image velocimetry system,'' Exp. Fluids, **25**, No. 4, pp. 316–319.
[10] Meinhart, C. D., Wereley, S. T., and Santiago, J. G., ''PIV measurements of a microchannel flow,'' Exp. Fluids, **27**, pp. 414–419.
[11] Tieu, A. K., Mackenzie, M. R., and Li, E. B., 1995, ''Measurements in microscopic flow with a solid-state LDA,'' Exp. Fluids, **19**, pp. 293–294.
[12] Meinhart, C. D., Barnhart, D. H., and Adrian, R. J., 1994, ''Interrogation and validation of three-dimensional vector fields,'' *Developments in Laser Techniques and Applications to Fluid Mechanics*, R. J. Adrian et al., eds., Springer-Verlag, Berlin, pp. 379–391.
[13] Westerweel, J., 1993, ''Efficient detection of spurious vectors in particle image velocimetry data,'' Exp. Fluids, **16**, pp. 236–247.